 doi:10.20944/preprints202008.0144.v1

Article

Chemo-stratigraphy, petrology and U-Pb geochronology of Karakılıçlı Volcanic Field in NW Anatolia: Implications for Hellenic Subduction System

Ali İskenderoğlu [1]* and Namık Aysal [2]

[1] Turkish Court of Accounts, İnönü Bulvarı, No: 45, 06520, Ankara, Turkey; ali.iskenderoglu@gmail.com
[2] İstanbul University – Cerrahpasa, Department of Geological Engineering, İstanbul, Turkey; aysal@istanbul.edu.tr
* Correspondence:Correspondence: ali.iskenderoglu@gmail.com

Received: date; Accepted: date; Published: date

Abstract: Western Anatolia comprises a vast amount of various volcanic successions spanning from Eocene to Upper Miocene periods. These units mainly display southward younging in broad sense and display large amounts of chemical variation that spanned from basalt to rhyolite. The southward younging of magmatism and chemical variations have been largely attributed to the retreat and roll-back of the Hellenic slab and the western escape of the Anatolian microplate. However, there is still a lack of high precision data to pinpoint the exact nature of the magmatism and lithospheric tectonics. In this contribution we investigated a poorly known region along the Western Anatolia along Manisa district called Karakılıçlı volcanic field. We investigated two different volcanic sections (Kalpakkaya and Çamlık hill) that display the best volcano-sedimentary features in terms of geochronology and geochemistry. Samples acquired from the bottom, middle and upper portions of these sections display Early-Middle Miocene ages of 17.64±0.20, 17.22±0.15, 16.16±0.17 and 16.36±0.13, 15.79±0.71 and 13.61±0.20 Ma respectively. The results indicate that the volcanism in the region generated by the melting of the mantle and/or lithospheric mantle by slab retreat and roll-back of the Hellenic slab and evolved in the shallow magma chambers/mushes by fractional crystallization, magma mixing and crustal assimilation.

Keywords: Western Anatolia 1; Geochronology 2; slab roll-back 3; Hellenic slab 4

1. Introduction

Western Anatolia comprise various magmatic units that mainly generated by the Aegean Subduction system during the Cenozoic period. First magmatic products of this system mainly generated at the Eocene time along the Biga Peninsula that compromise both plutonic and volcanic products. By the large scale roll-back of the subducted Hellenic slab, the magmatic units also shift to the much southerly areas till the recent [1]. The generation of the first products of the Eocene magmatism highly debated and several hypotheses postulated such as subduction related generation, arc-continent collision and post-collisional magmatism related generation [2,3,4,5,6]. After that period, Oligo-Miocene and Mio-Pliocene magmatism became more pronounced. During these time intervals, coevally generated calc-alkaline, high K volcanics and I-type plutonics cover the wide areas of the Western Anatolia. Magmatic products (Figure 1) generated during these time periods (termed as display vast amount of chemical heterogeneity that mainly generated by the shallow seated magma chamber processes (e.g. fractional crystallization, magma mixing/mingling, crustal assimilation) that alter the original source chemistry [7,8,9,10].

Preprints (www.preprints.org) | NOT PEER-REVIEWED | Posted: 6 August 2020 doi:10.20944/preprints202008.0144.v1

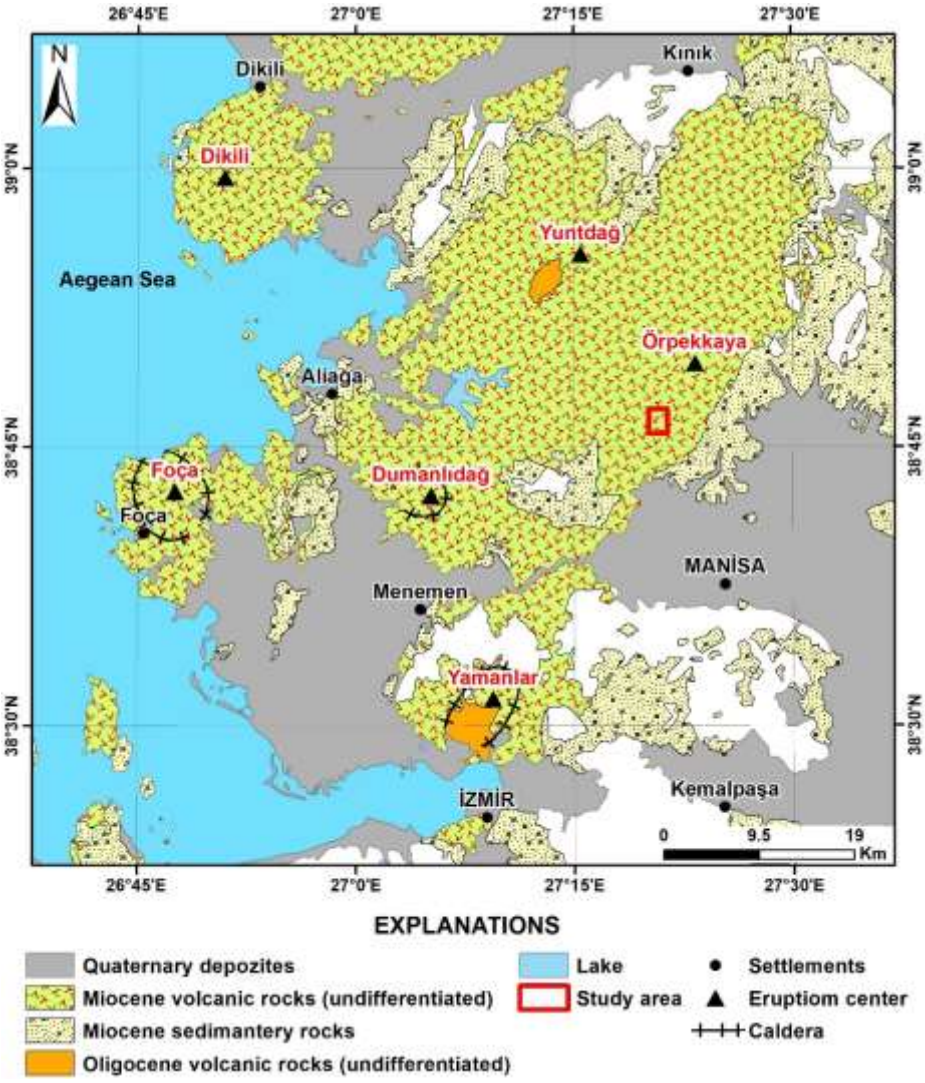

Figure 1. Distribution of Oligocene – Miocene volcanic rocks in Western Anatolia (simplified from MTA 1/500.000 scaled geology map).

Volcanic products in that period often intercalated with the sedimentary products that generated in sub-aerial conditions and cover large tracts [11,12,13,14]. In the meantime, these time corresponding to a period before a major shift on the tectonic development in the Western Anatolia such as exhumation of the core complexes [1,13,14,15,16,17,18,19,20], generation of the asthenosphere derived alkaline volcanism [21,22] and generation of the İzmir-Balıkesir Transfer Zone [12,13,23,24]. However, there is still lack of data for the Miocene time interval in the region.

In order to better characterize the major changes in that period, we select two section of Miocene volcano-sedimentary around the Western Anatolia Volcanic Province (WAVP) which is crops out along the Karakılıçlı field of Manisa district (Figure 2). These sections situated at the Kalpakkaya Hill and Çamlık Hill areas, the volcano-stratigraphic sections logged, they are sampled from bottom to top and whole-rock geochemistry analysis have been done on different lava flows and pyroclastic units. In addition to that, from U-Pb zircon age determinations have been conducted on lower, middle and upper portions of these two stratigraphic column in order to understand the spatial and geochemical evolution of the volcanism. The chemo-stratigraphy sections have been constructed in order to understand petrological evolution on the Miocene volcanism and their regional magmatic implications on the Hellenic subduction system. The output of this work will put new constrains on the evolution of both magmatic evolutions the Aegean region and both the melting, assimilation storage and homogenization (MASH) processes.

 doi:10.20944/preprints202008.0144.v1

2. Materials and Methods

2.1. Zircon U-Pb LA-ICP-MS Geochronology

Six different samples have been selected from the different layers of the two measured section (three sample per each section) in order to understand the spatial and geochronological evolution of the volcanism in the region. In each sample, 2 kg of samples have been crushed in mill and their grain size reduced below the 250 micron. The sample size of 63 to 250 micron has been selected and separated by magnetic separator and heavy liquid (sodiumpolytungstate) to acquire the zircon minerals. The finally the samples found under binocular microscope and embedded in the epoxy resins. The resins polished and imaged by the optical cathodoluminescent Citl CL8200 Mk5-1 at the Istanbul Technical University Geochemical Analysis Laboratories (ITU-JAL). By the guide of these images, specific spot has been selected for geochronology analysis. Zircon U-Pb analysis have been conducted in Geochronology and Geochemistry Laboratory of Istanbul University-Cerrahpaşa Geological Engineering Department by the NexION 2000 ICP-MS combined with the ESI NWR-213 solid phase laser. The spot sized dispersed between 20 to 45 micron and helium has been used as a carrier gas (0.5 lt/sn). Zircon reference material 91500 has been as a primary and AusZ-10 and MudTank have been used as a secondary reference material. All the measurements evaluated by the Iolite software version 2.5 [25].

2.2. Whole-rock Geochemistry

Twenty-three samples have been selected for the whole-rock geochemistry analysis that represent the two different stratigraphic section. The major oxide analysis of these samples have been analyzed by the X-ray fluorescence (XRF) spectrometer (Bruker S8 Tiger Wavelength Dispersive XRF) at the Geochemistry Analysis Laboratory of Istanbul Technical University (ITU-JAL). The major oxide values have been analyzed on samples which turn into fused glass discs that created by the lithium tetraborate/metaborate fusion in the platinum-golden crucibles. The loss on ignition values of these values calculated separately. The trace and rare element values of these samples have been measured by the Perkin Elmer ELAN DRC-e instrument at (ITU-JAL) and Thermo XSeries II ICP-MS instrument at the geochemistry laboratory of Mineral Exploration Research Headquarters of Turkey.

3. Results

3.1. Geological Setting and Petrography

The study area croups out along the basement units of Bornova Flysch Zone which is situated between the Menderes Massif and the Sakarya Zone (Figure 1, [26,27]. Bornova Flysch Zone consists Mesozoic limestone blocks, mafic volcanics, radiolarites and serpentinite blocks that embedded in a highly deformed sedimentary matrix [28,29]. There are three main volcanic edifices have been found in the region that called Yamanlar, Dumanlıdağ and Yuntdağı volcanoes [30,31,14]. The base of the Miocene volcanism started with a thick pyroclastic section that is called Foça Tuff. This unit contain white-yellowish ignimbrites and sporadic rhyolitic plugs which are intercalated with lacustrine clay stones and limestone units [32,33,34]. This unit overlain by Hasanlar volcanics [32,35] that contain volcanic ash, block, lava breccia, tuff and lenticular limestone units together with more prominent basalt and pyroxene-andesite lavas [34,35]. Through the upper portion of the stratigraphy, Early-Middle Miocene aged Dumanlıdağ and Yuntdağı volcanics getting prominent and became the most widespread volcanic product around the region [36,37,38,39]. Yuntdağı volcanics represented by sub-units of Rahmanlar pyroclastics [36] and Akçaköy ignimbirite member [37,38]. All these units are intercalated with Middle-Upper Miocene sub-aerial and lacustrine sedimentary successions [32,37,11].

Preprints (www.preprints.org) | NOT PEER-REVIEWED | Posted: 6 August 2020 doi:10.20944/preprints202008.0144.v1

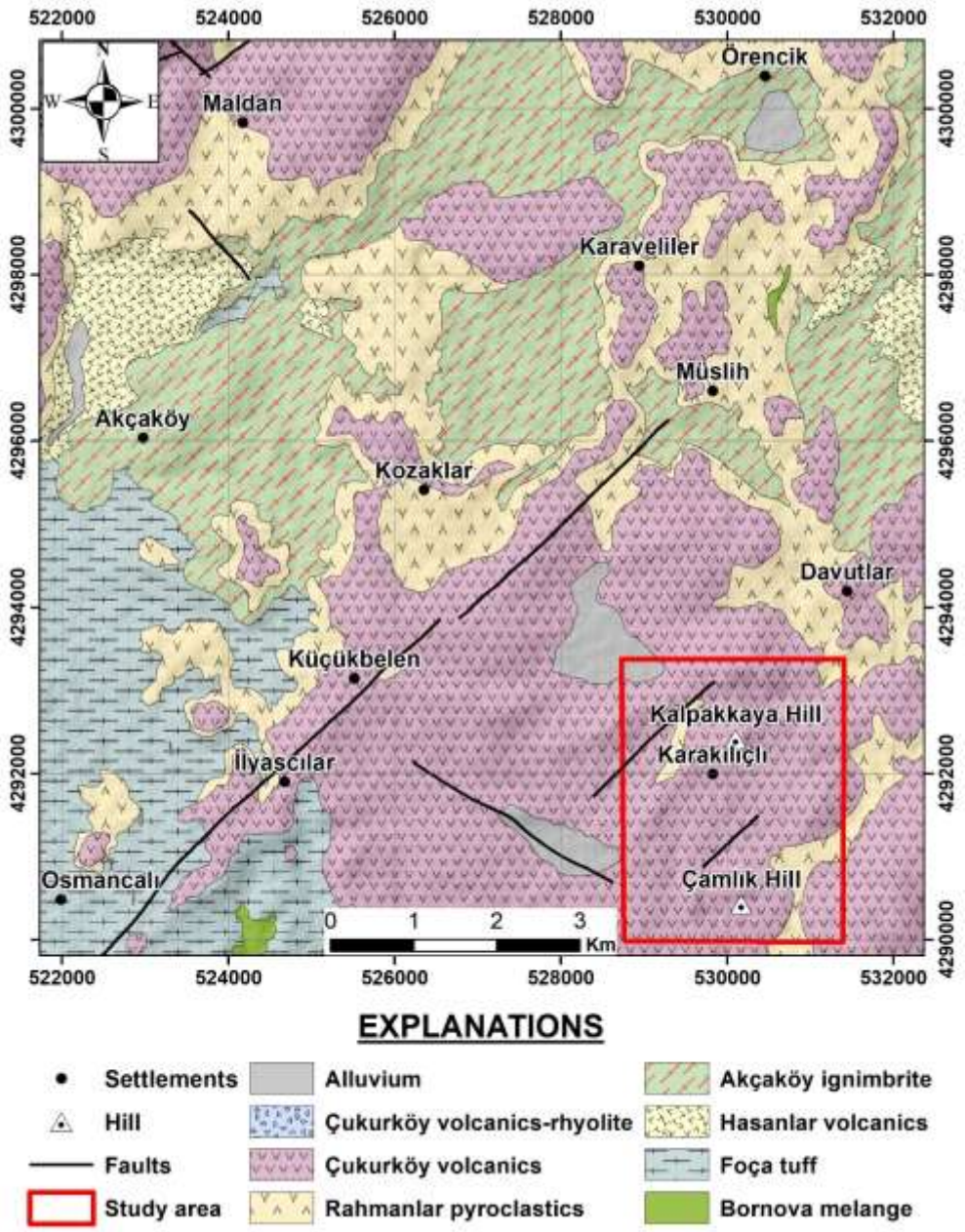

Figure 2. Geological map of the study area (Adopted from [38,39], coordinate system: WGS1984_UTM_Zone35N).

Dumanlıdağ Volcanics which is the stratigraphic equivalent of the Yuntdağı volcanics, represented by Çukurköy sub-unit in the study area [32,37,40,41]. Çukurköy volcanics consists of grey and reddish andesite, dacite, rhyodacitic lavas and pyroclastic interlayers. Lavas mainly display porphyritic, microlithic and vitrophyric textures and mainly contain plagioclase, biotite, hornblende, pyroxene and a small amount of sanidine [30]. Flow banding is common and thorough the upper portion of the sections glassy flow foliation became dominant. The two different volcano-sedimentary sections related to Yuntdağ volcanites which are named Kalpakkaya Hill and Çamlık Hill have been measured that the characteristics of the volcanic successions were best preserved (Figure 3). Kalpakkaya Hill section has been started with reddish-grey porphyrithic dacitic lavas from the bottom. The section continiues with porphyric textured and banded dacitic lavas that consists thin tuff interlayer. The section continues monotonously and display approximately 250-meter thickness. On the other hand, Çamlık Hill started with porphyrithic dacitic lavas with pyroclastic inliers in the bottom and overlain by porphyric and banded dacitic units, contrary to Kalpakkaya Hill section, the reddish brown and grey andesitic lavas situated at the top of the section (Figure 3).

Preprints (www.preprints.org) | NOT PEER-REVIEWED | Posted: 6 August 2020 doi:10.20944/preprints202008.0144.v1

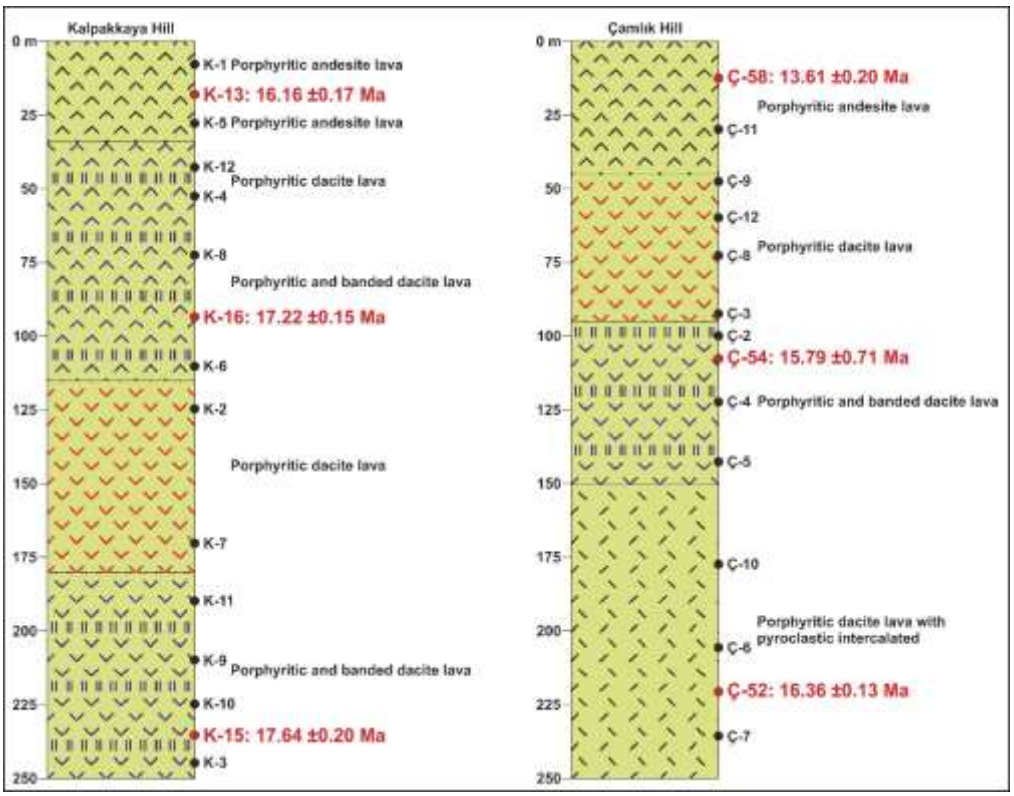

Figure 3. Stratigraphic columnar sections of Kalpakaya and Çamlık Hills. Red points represent dated samples and black points represents the samples obtained for the whole-rock geochemistry analysis.

3.2. Zircon U–Pb crystallization ages

The selected zircons mainly show transparent, pale yellow colors and display prismatic features. CL images mainly display magmatic zoning and generally homogeneous features. The results of the zircon crystallization ages for the Kalpakkaya and Çamlık Hill sections (three samples from lower, middle and upper levels per each section) have been outlined below.

3.2.1. Section of Kalpakkaya Hill

Sample K-15 (lower part): The 206Pb/238U ages obtained from the K-15 samples display ages dispersed between 18.73 ± 0.48 Ma to 17.12 ± 0.35 Ma (Supplementary Table 1a). Besides, the concordia age calculated as 17.64 ± 0.20 Ma and the mean age deduced as 17.68 ± 0.23 Ma (Figure 4a).

Sample K-16 (middle part): The 206Pb/238U ages obtained from the K-16 sample display ages dispersed between 18.73 ± 0.45 Ma to 16.35 ± 0.61 Ma (Supplementary Table 1b). Besides, the concordia age calculated as 17.22 ± 0.15 Ma and the mean age deduced as 17.29 ± 0.26 Ma (Figure 4b).

Sample K-13 (upper part): The 206Pb/238U ages obtained from the K-16 sample display ages dispersed between 18.99 ± 0.84 Ma to 13.07 ± 1.16 Ma (Supplementary Table 1c). Besides, the concordia age calculated as 16.16 ± 0.17 Ma and the mean age deduced as 16.22 ± 0.55 Ma (Figure 4c).

3.2.2. Section of Çamlık Hill

Çamlık Hill section display quite similar age population like the Kalpakkaya Hill section.

Sample C-52 (lower part): The 206Pb/238U ages obtained from the C-52 sample display ages dispersed between 18.02 ± 0.35 Ma to 15.52 ± 0.42 Ma (Supplementary Table 1d). Besides, the concordia age calculated as 16.36 ± 0.13 and the mean age deduced as 16.44 ± 0.25 Ma (Figure 4d).

Sample C-54 (middle part): The 206Pb/238U ages obtained from the C-52 sample display ages dispersed between 18.86 ± 0.64 Ma to 14.22 ± 0.35 Ma (Supplementary Table 1e). Besides, the concordia age calculated as 15.79 ± 0.71 and the mean age deduced as 15.9 ± 1.1 Ma (Figure 4e).

Preprints (www.preprints.org) | NOT PEER-REVIEWED | Posted: 6 August 2020 doi:10.20944/preprints202008.0144.v1

Sample C-58 (upper part): The 206Pb/238U ages obtained from the C-58 sample display ages dispersed between 14.75 ± 0.48 Ma to 11.59 ± 0.74 Ma (Supplementary Table 1f). Besides, the concordia age calculated as 13.61 ± 0.20 and the mean age deduced as 13.69 ± 0.47 Ma (Figure 4e).

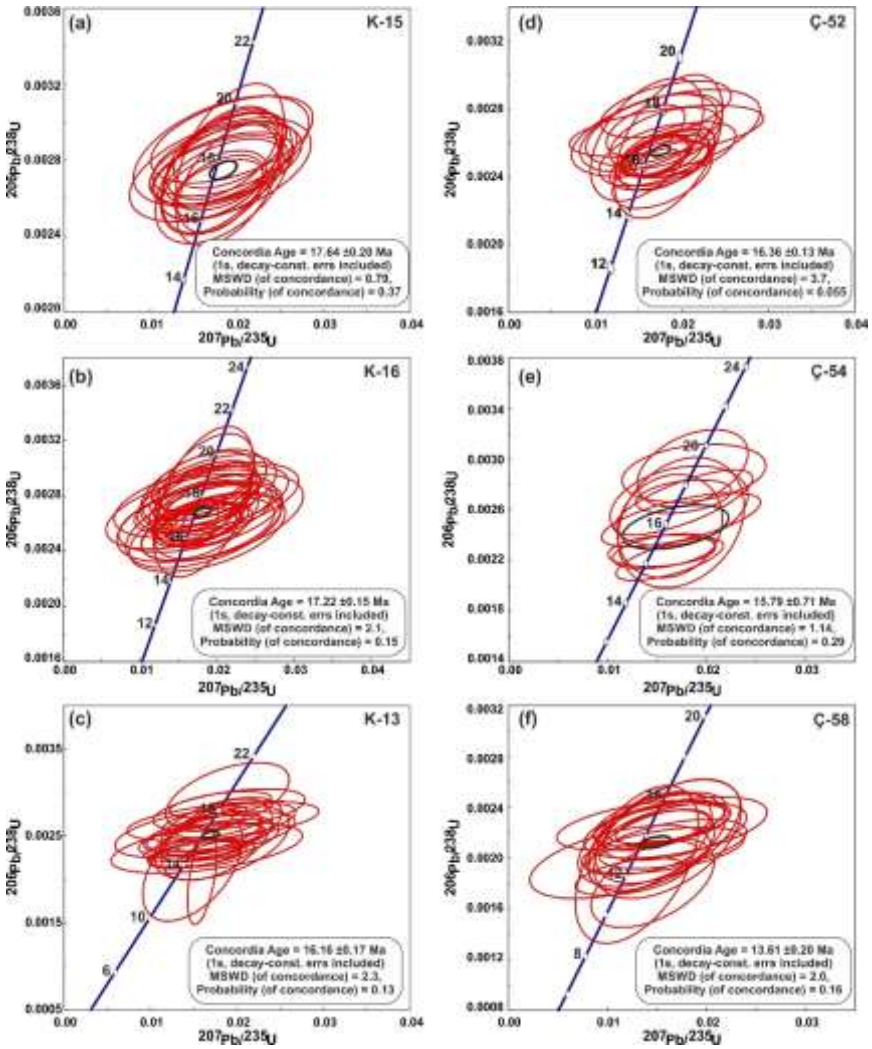

Figure 4. Zircon U-Pb concordia diagrams of Kalpakkaya Hill and Çamlık Hill volcanic sections. Figure (a) and (d) are corresponding to lower parts, (b) and (e) are corresponding to middle parts and (c) and (f) are corresponding to upper parts of the sections.

3.3. Major and trace elements

The results of the major oxide and trace element analysis of twenty-three samples from Kalpakkaya and Çamlık Hill have been giving in Supplementary Table 2. These volcanic rocks show narrow SiO_2 contents ranging from 61.70 to 66.53 wt.%, TiO_2 from 0.68 to 0.85 wt.%, Al2O3 from 13.88 to 16.77 wt.%, Fe_2O_3 from 4.48 to 6.19 wt.%, MgO from 1.10 to 2.28 wt.%, CaO from 2.86 to 5.80 wt.%, Na_2O from 2.39 to 3.36 wt.% and K_2O from 2.94 to 3.80 wt.% (Table 3). Na_2O/K_2O ratios of the Kalpakkaya Hill volcanic units dispersed along 1.02 to 1.10 and slightly show sodic character, while Çamlık Hill volcanic units display much lower Na_2O/K_2O ratios and have a much potassic character. Magnesium number of the samples dispersed 30 to 49 (Mg# =100 x molar Mg / (Mg+Fe)).

The results of the analysis plotted at the discrimination diagrams. On the Zr/TiO_2 vs. SiO_2 diagram, [42] the studied units mainly plot along the dacite-rhyodacite fields sub-ordinately they dispersed along the andesite field (Figure 5a). On the K_2O vs. SiO_2 diagram [43], all the samples straddled along the high - K calc-alkaline series (Figure 5b).

Preprints (www.preprints.org) | NOT PEER-REVIEWED | Posted: 6 August 2020 doi:10.20944/preprints202008.0144.v1

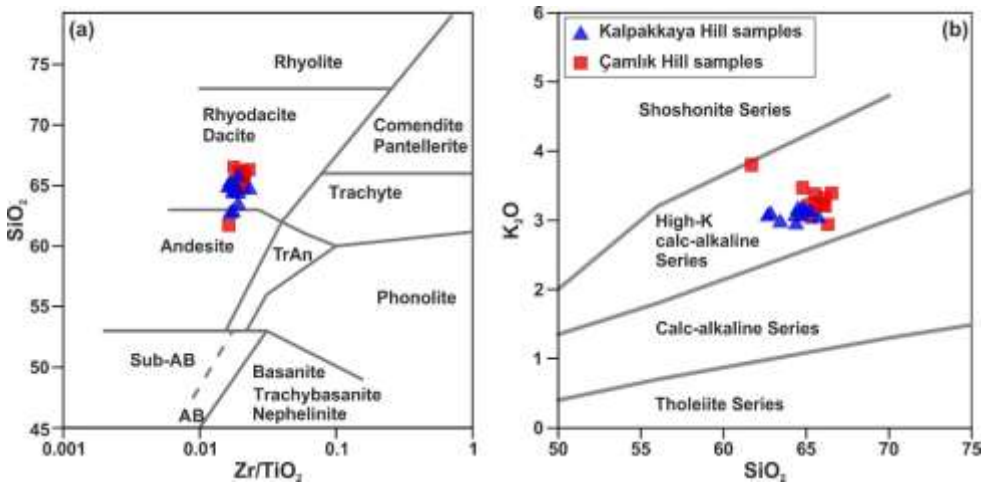

Figure 5. a) Zr/TiO_2 vs. SiO_2 [42], and b) K_2O vs. SiO_2 discrimination diagrams [43] for the classification of volcanic rocks.

4. Discussion

4.1. Whole-rock chemistry and chemo-stratigraphy

The lava flows from Kalpakkaya and Çamlık Hill sections mainly display intermediate dacitic and andesitic chemistry. The Harker variation diagrams can be used to assess various magmatic evolutionary stages such as fractional crystallization, mixing, assimilation and replenishment. SiO_2 vs TiO_2, Al_2O_3 and Fe_2O_3 variation diagrams imply mainly fractional related evolutionary trends with the increasing silica content despite a bit scattering. On the other hand, SiO_2 vs MgO, CaO, Na_2O, K_2O, Sc and Co diagrams show much wider scattering. Besides, for the other elements such as Ba, Rb, Sr and Y the evolutionary trends generally show flat trends which are supportive for continuously replenished and/or possibly mixed with a much mafic magma throughout the generation of the volcanism. Despite the fact that the Harker diagrams give valuable insights about the evolutionary stages of the magmatism, it is not always easy to track the temporal changes of the magmatism just by interpreting the different phases and events in the Harker trends.

In order to better constrain the temporal and geochemical changes of the volcanic sections of Kalpakkaya and Çamlık hill, the lava and tuff samples obtained from different levels of the section (lower-middle-upper) were analyzed, and the obtained results plotted against the height in the stratigraphic column to reveal the chemical stratigraphy of the volcanism throughout the time. When the measured volcanic levels are correlated with the stratigraphic height and major oxide chemistry for the both sections (Figure 7, 8); the SiO_2 content of the both sections getting decreased throughout the stratigraphic column and the lower levels of the sections imply a possible magma mixing event by the behavior of the major oxides such as general increase of MgO contents. Similarly, some of the major oxides display prominent peaks but mainly display straight through the upper portion of the stratigraphic columns.

Preprints (www.preprints.org) | NOT PEER-REVIEWED | Posted: 6 August 2020 doi:10.20944/preprints202008.0144.v1

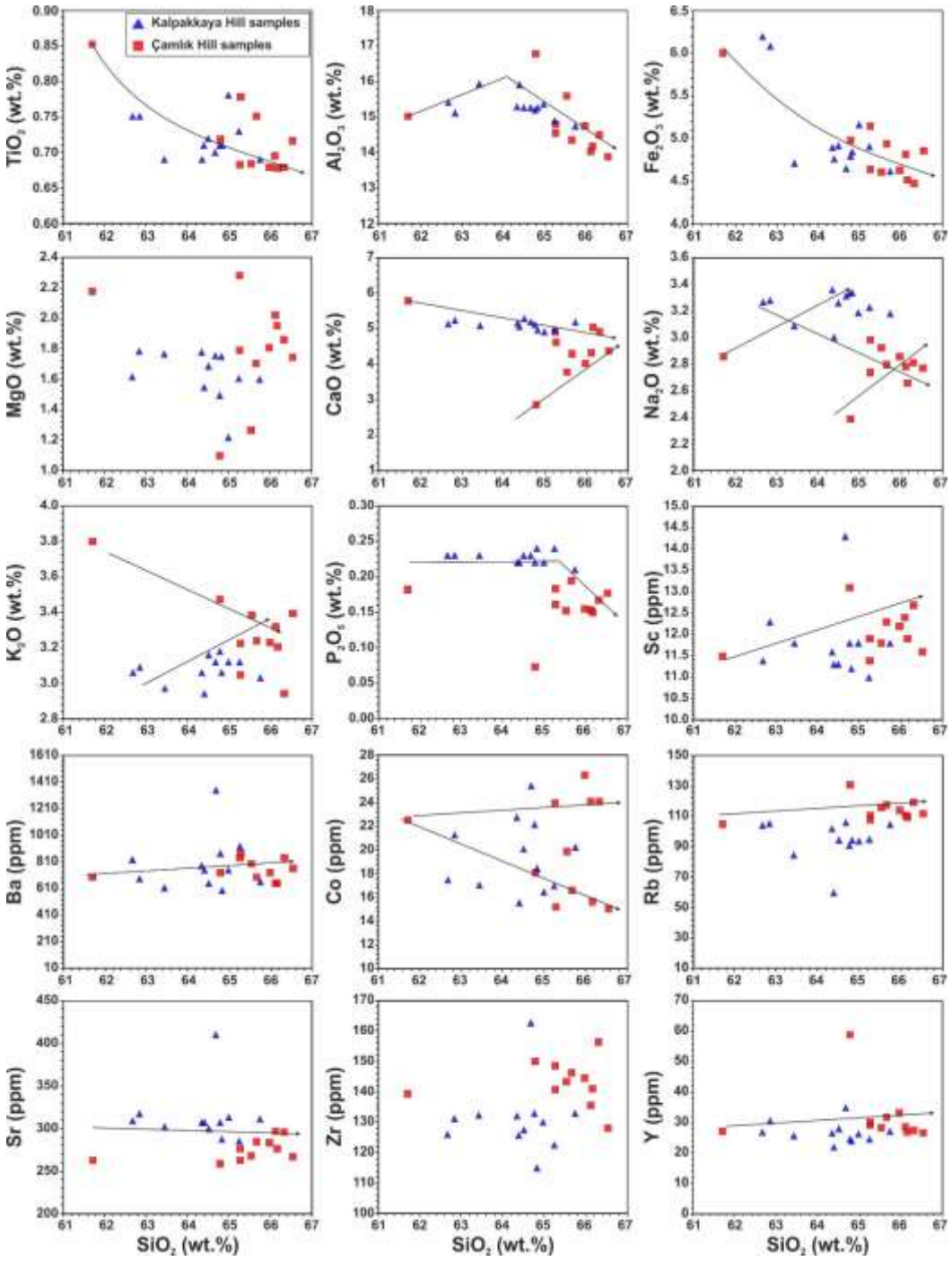

Figure 6. Harker variation diagrams for the SiO_2 vs different major oxide and selected trace elements.

Preprints (www.preprints.org) | NOT PEER-REVIEWED | Posted: 6 August 2020 doi:10.20944/preprints202008.0144.v1

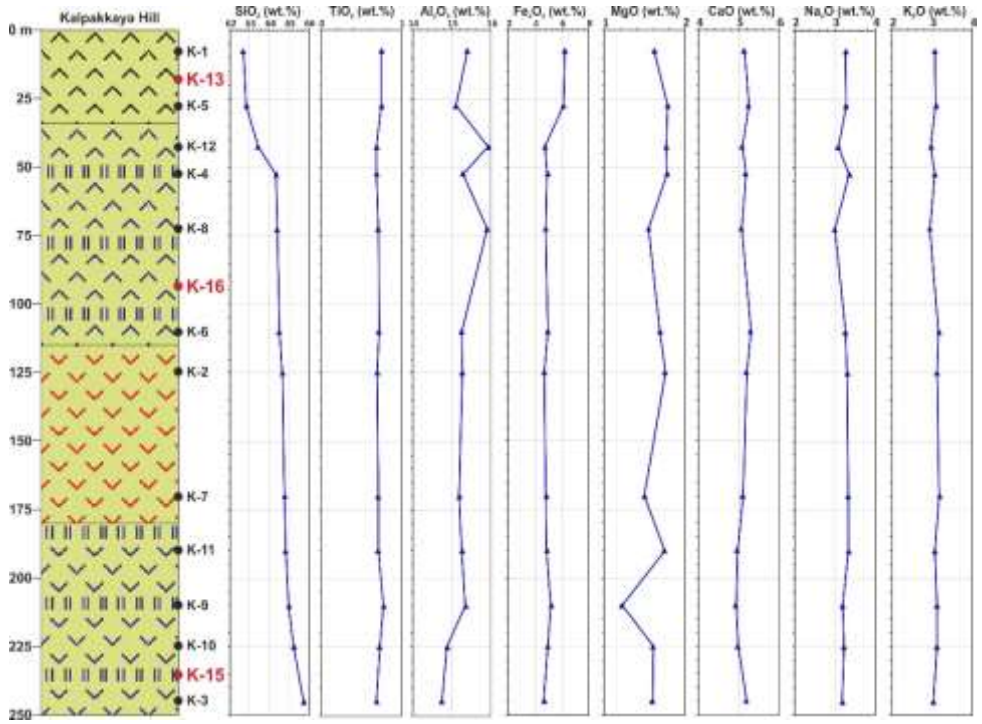

Figure 7. Chemical-stratigraphy of the Kalpakkaya Hill volcanics based on the major oxide chemistry.

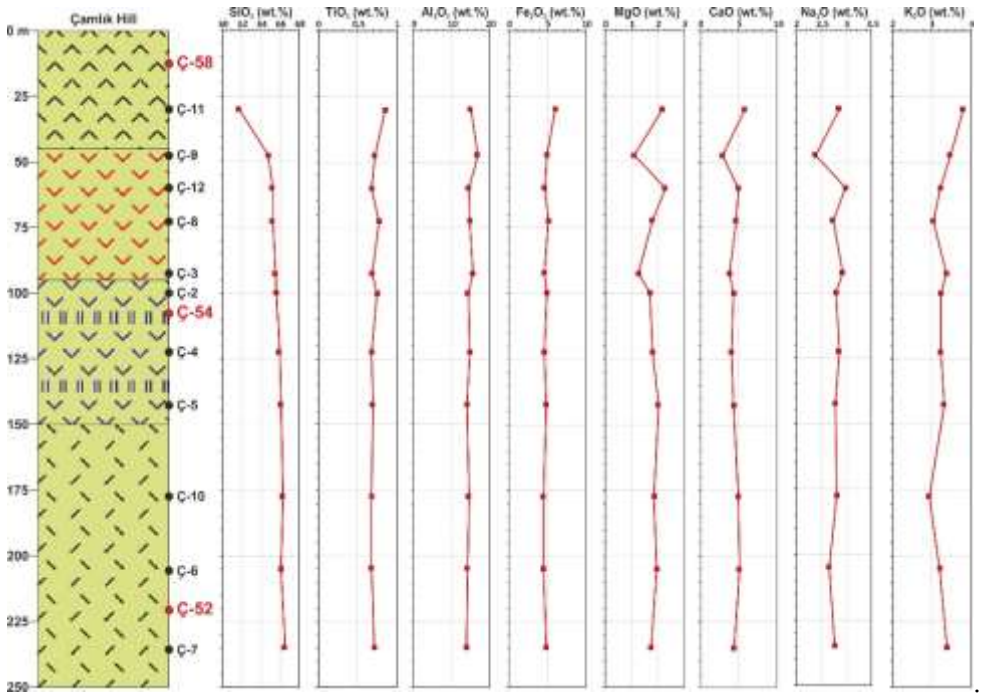

Figure 8. Chemical-stratigraphy of the Çamlık Hill volcanics based on the major oxide chemistry.

On the chemical stratigraphy of the Kalpakkaya and Çamlıktepe volcanics (Figure 9, 10), it is observed that the trace elements (Sc, V, Co, Ba, Rb, Sr, Nb and Zr) follow a linear enrichment trend towards the middle levels of the section. Sc, V and Co elements mainly used to assess the evolution of the crystallization processes and they mainly diminished in the magma chamber throughout the evolutionary stages from mafic to silica transition. Ba, Rb and Sr are mainly used to track the behavior of the feldspar crystallization and they tend to getting higher with the increasing silica content. Rb together with Nb also used to assess the behavior of the mica phases and getting increased with the increasing silica. Similar to these elements, Zr tends to getting increasing with the increasing silica and used to assess the behavior of the accessory phases such as zircon, apatite or monazite. Similarly,

Preprints (www.preprints.org) | NOT PEER-REVIEWED | Posted: 6 August 2020 doi:10.20944/preprints202008.0144.v1

like the major oxide data, trace element variation in the measured sections show the chemistry of the lavas did not change significantly through their temporal evolution. Observations made in parallel with the 3 million years' evolution of the chemo-stratigraphy and nearly similar magma composition imply that the magma evolution might experience (i) continuous supply of a more mafic magma to balance the fractional crystallization related evolution; (ii) homogenization of mafic and intermediate magma throughout the evolution of volcanism and/or generation within an open system magma chamber. Hence, the mainly similar magma chemistry during the evolution of the magmatism supportive for a large magma chamber that created big caldera events also described in the nearby regions [14,44] and thereby the different explosive events recorded in the area did not significantly affect the magma composition.

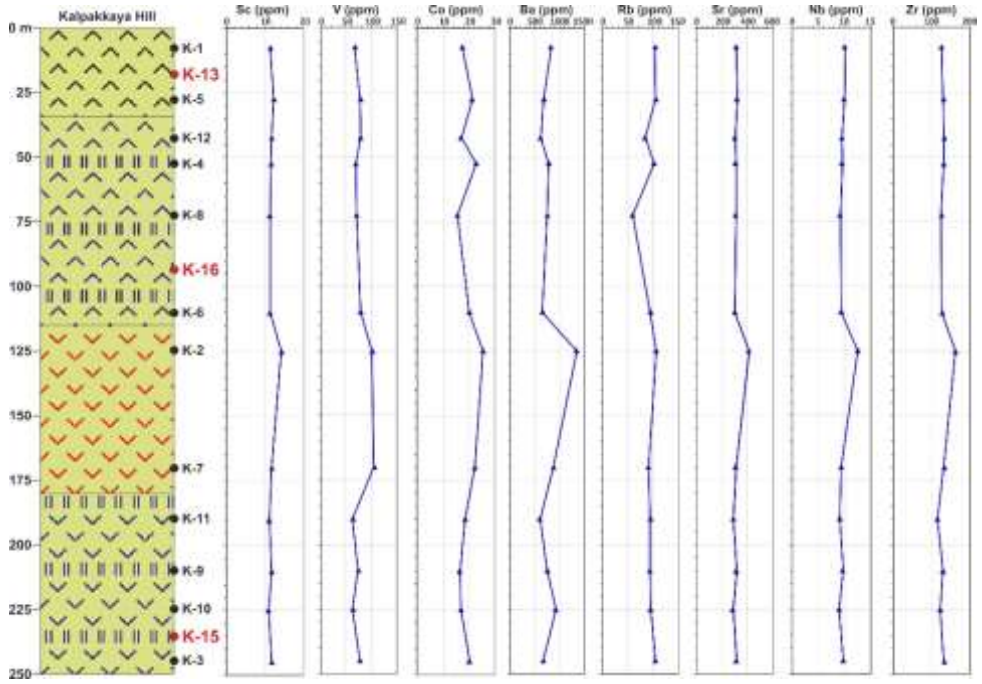

Figure 9. Chemical-stratigraphy of the Kalpakkaya Hill volcanics based on the trace elements.

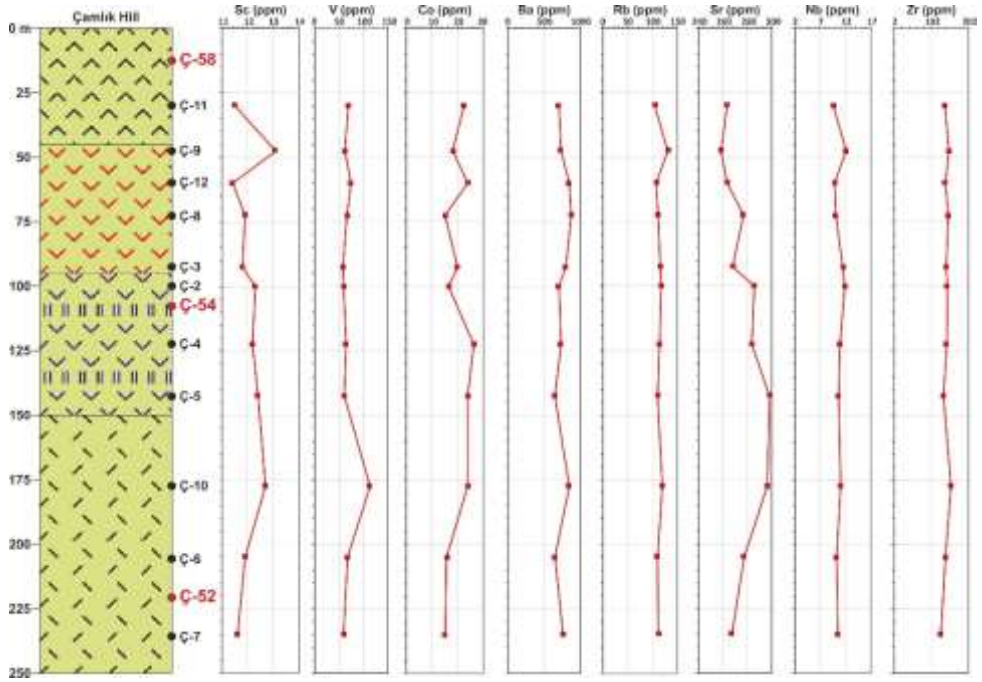

Figure 10. Chemical-stratigraphy of the Çamlık Hill volcanics based on the trace elements.

 doi:10.20944/preprints202008.0144.v1

4.2. Petrogenesis of Volcanic rocks

Several different models have been created by using the geochemistry results obtained from Kalpakkaya and Çamlık Hill volcanics in order to understand the magma chamber/mush processes. We use the FC-Modeler algorithm of Keskin (2002) [45] to model the fractional crystallization processes by using the Sr/Rb vs Sr. For modeling parameters, Kd values compiled from GERM database and literature which are embedded in the FC-Modeller program have been used. For plagioclase, sanidine, hornblende, biotite and zircon, particularly intermediate and acidic values are selected and crystallization vectors created.

The calculated crystallization vectors show that the plagioclase, sanidine and biotite crystallization is the dominant process while the amphibole and zircon crystallization is less prominent. To reveal the magma mixing and replenishment processes, creating a binary diagram that consists of a compatible vs. an incompatible element can give valuable insights about the magma evolution. To reveal the possible mixing events, we created Co vs. Th diagram to track the possible mixing traits. If there is common fractional crystallization related processes occurred, our samples will align along the FC-1 and FC-2 curves on the Figure 11b. On the other hand, if the magmatic system is open and mixing or replenishment processes happened, the plotted samples should be aligned along the straight lines. When we check the plotted samples, some portion of our volcanic units follow the curved lines of FC-1 and FC-2, while a significant amount of the samples plotted along the straight lines which support the possible existence of the magma mixing processes (mixing of mafic and felsic members) through the evolution of the volcanism (Figure 11b).

Even though the fractional crystallization and magma mixing processes affected the magma chemistry in our samples, crustal assimilation can also effect the magmatic processes since our volcanic units display high silica contents. To reveal the possible assimilation processes, we use the assimilation-fractional crystallization algorithms of the DePaolo (1981) [46] that implement to the excel spreadsheet AFC-Modeller software by Keskin (2013) [47]. We specifically select Ta/Zr and Zr values. The Ta/Zr ratios are used as an assimilation index while Zr values interpret as a fractionation index (Figure 11c). For modeling scheme, we use the upper-crustal values of Taylor and McLennan (1985) [48] for an assimilant, and a calc-alkaline basalt from the Çanakkale-Kirazlı region selected as basic end member (BEM) for the primitive lava composition (unpublished data; Zr: 84.4 ppm and Th: 4.50 ppm). The calculated trajectories show that volcanic units plotted along a linear array from the BEM to assimilant. Zr values in our samples display quite similar values which can be interpreted as the assimilation is much more prominent regarding to the fractionation related processes (r (Ma/Mc) = 0.4 – 0.7). When the all the geochemical data and modeling experiments interpreted, it can be postulated that the assimilation and magma mixing related processes are much more prominent comparing to the fractional crystallization related modifications, and/or possible continuous infiltration of the mafic or much primitive magma to the much felsic shallow seated magma chamber/mush to maintain the similar magmatic character.

Preprints (www.preprints.org) | NOT PEER-REVIEWED | Posted: 6 August 2020 doi:10.20944/preprints202008.0144.v1

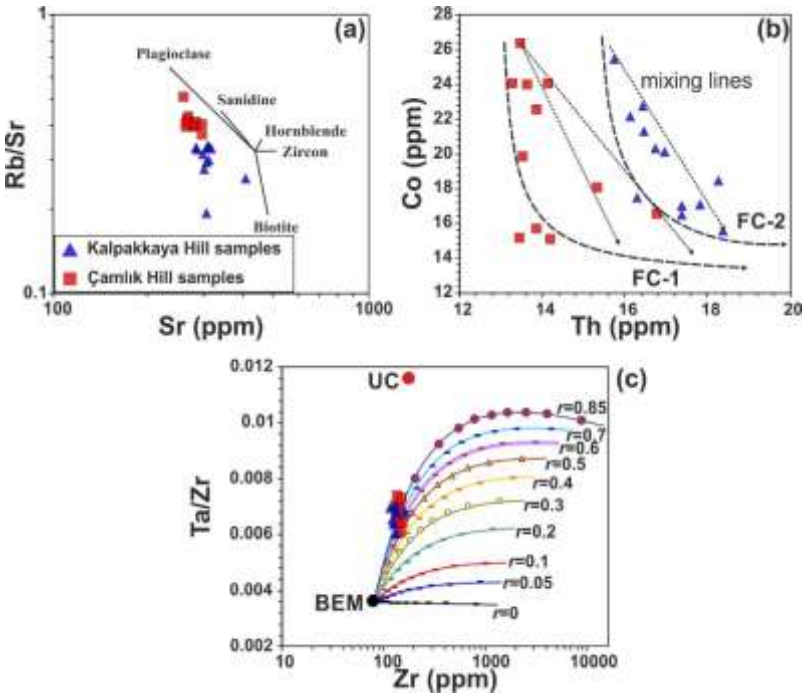

Figure 11. Several different magma modeling experiments have been done on the Kalpakkaya and Çamlık hill volcanics to reveal the magma chamber/mush dynamics.

Selected samples have been plotted on the N-type MORB normalized spider diagrams to understand the geochemical characteristics of the magmatism. In these diagrams, all volcanic units display apparent enrichment in LILEs (Large Ion Lithophile Elements; Sr, K, Rb, Ba, Th) and much lower but stil prominent enrichment in LREEs (Light Rare Earth Elements; La, Ce and Nd). On the other hand, HFS (High Field Strenght) elements (Tb, Ti, Y and Yb) show apparent depletion (Figs. 12a-b). There is clear depletion through Th to Ta and Nb and a similar depletion also be found through La to Nd (Fig 12). Besides Hf-Zr-Sm elements display nearly flat patterns (Figure 12a, b). Even the Nb-Ta display very apparent depletion relative to the neighboring elements, they still enriched relative to the N-MORB values (Figure 12a, b). The apparent Nb-Ta anomaly mainly attributed to the subduction related arc environments while it can have generated by the relict metasomazited portions generated in the collision related crustal-lithospheric environments.

Chondrite normalized rare-earth element (REE) variation diagrams of the volcanic units display similar patterns for all series. In the selected units of the both volcanic sections, light rare earth element (LREE) of the samples display relative enrichment regarding to the other elements and the majority of the heavy light rare earth elements (HREE) display similar values to the chondrithic values (Figure 12c,d). Besides in all series there is an apparent negative Eu anomaly (Eu/Eu* ratios ((Eu)cn/[(Sm)cn x (Gd)cn]0.5 cn stands for chondrite normalized) dispersed between 0.62 to 0.75). Also most of the middle rare earth elements show relative depletions comparing to the LREE and HREE. Thus this features support the amphibole and feldspar fractionation of the studied volcanic units.

In tectonic discrimination diagrams of Pearce et al., (1984) [50] that using Nb vs Y values, our samples plotted along the volcanic arc granites (VAG) and syn-collisional granite field and one samples plotted along the within-plate field (Figure 13a). At the tectonic discrimination diagram of Harris et al., (1986) [51] that utilizing Rb/30 -Hf- 3xTa; our samples dispersed along the volcanic arc and late and post-collisional fields (Figure 13b). The Th/Yb vs. Ta/Yb [52] and Th/Yb vs. Nb/Yb diagrams [53] reveal that the volcanic units generated along the active continental margin and volcanic arc environment. These diagrams imply that the magma source area of the studied volcanic samples effected by the subduction related modifications and possibly effected by crustal related modifications.

Preprints (www.preprints.org) | NOT PEER-REVIEWED | Posted: 6 August 2020 doi:10.20944/preprints202008.0144.v1

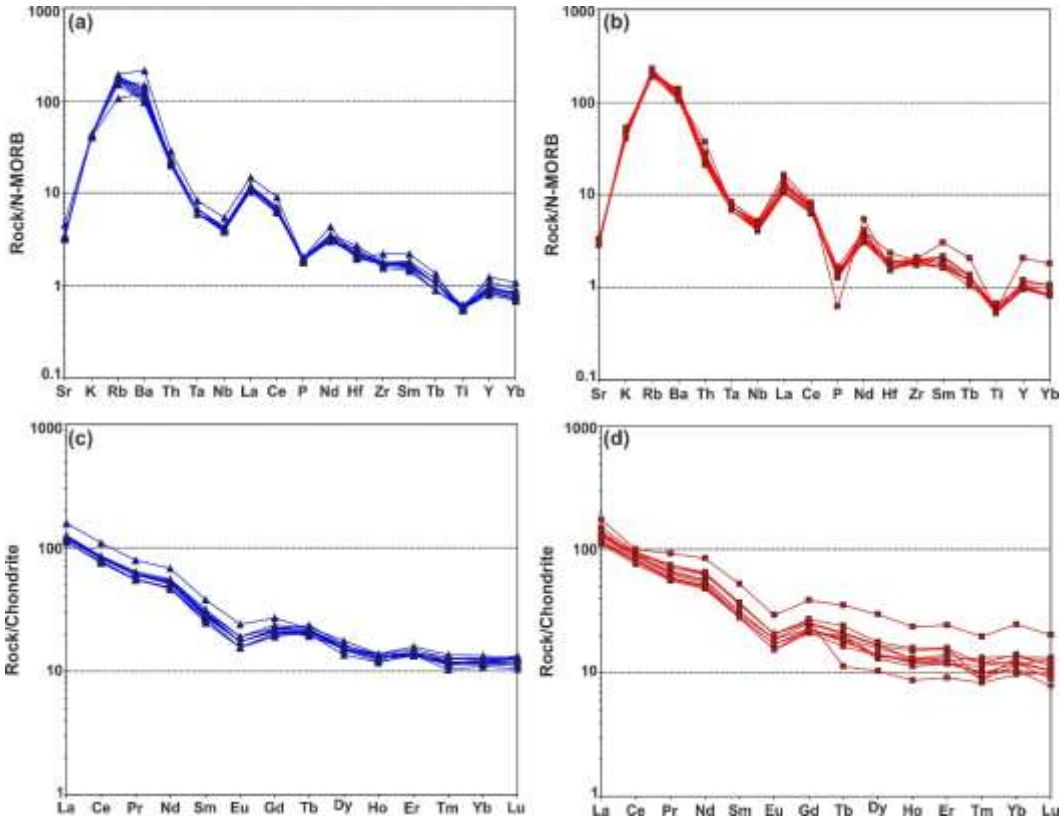

Figure 12. N-MORB (a, b) and chondrite (c, d) normalized spider diagrams of Kalpakkaya hill (a, c) and Çamlık Hill (b, d) samples [49].

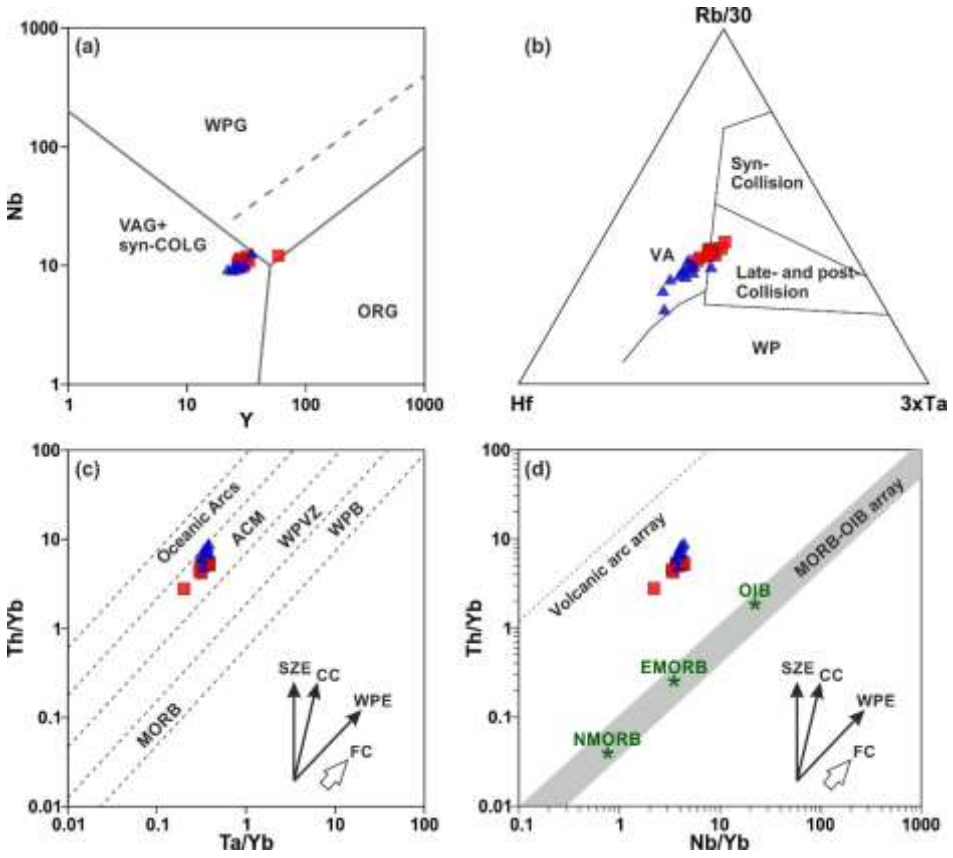

Figure 13. Tectonic discrimination diagrams of a) Nb vs. Y [50], b) Rb/30-Hf-3xTa [51, Th/Yb vs. Ta/Yb [52] and Th/Yb vs. Nb/Yb [53].

Magma source chemistry, volcano plumbing system and petrogenetic-geochronologic evolution of the study area and environs have been investigated by different studies in the literature [54,55,41,30,31,14,44,33,34,56,23]. The major portion of these studies imply that the volcanic and plutonic units in that region generated by the fractionation, assimilation and magma mixing processes of the shallow seated magma batches that generated from the lithospheric mantle and mantle domains [8,12,57]. The studies have been conducted in the recent years imply that the Cenozoic magmatism in the Western Anatolia mainly controlled by the slab retreat and the roll-back. Different studies imply that the Early-Middle Miocene magmatism in the region generated by the roll-back and rotation of the Hellenic slab, thinning of the continental crust, rupturing of the slab and transfer faults and block rotations in the upper crust control the pathways of the magma intrusive systems [14,44,33,56,23]. In a similar manner, different studies suggest that the roll-back of the Hellenic slab to the south/southeast through time also control the spatial-temporal and geochemical character of the magmatism in the region [54,58,59,18,60,14,10,57].

Our result supports a similar generation for the volcanic units in the Karakılıçlı field volcanic units that we check and evaluate two different chemo-stratigraphical section. Our data imply that volcanism in Karakılıçlı field fed by shallow seated magma chamber/mush that marked by fractional crystallization, magma mixing and assimilation related processes. Even though the complex shallow seated processes completely masked the original source chemistry, we tentatively postulated that our units possibly derived from melting of the mantle and/or subcontinental lithospheric mantle regions that triggered by the roll-back and rotation of the Hellenic slab during the Miocene pceriod.

5. Conclusions

The studies conducted in Karakaçlı volcanic field that mainly focused on Kalpakkaya and Çamlık Hill section show that the volcanic units in the region mainly represented by dacitic, rhyodacitic and andesitic lavas and tuff which are intercalated with the sporadic Neogene sedimentary units. The studied volcanic units generated by the large caldera event that created the Yuntdağı volcanism.

Zircon U-Pb LA-ICP-MS ages indicate that the Kalpakkaya Hill section show 17.64 ± 0.20, 17.22 ± 0.15 and 16.16 ± 0.17, Ma ages from bottom to top and Çamlık Hill section display 16.36 ± 0.13, 15.79 ± 0.71 and 13.61 ± 0.20 Ma (Lower – Middle Miocene) ages which are compatible with the existing age data acquired around the region.

Geochemistry of the units mainly shows high-K calc-alkaline character and display volcanic arc and post-collisional tectonic settings. Major oxide and trace element behaviors indicated that the volcanism sourced from mantle and/or lithospheric mantle mafic melt that heavily masked by fractional crystallization, magma mixing and crustal assimilation. The chemo-stratigraphy sections imply that the geochemical character of the samples did not change temporally, magma mixing of felsic crustal melts and much mafic inputs is the dominant processes and fractional crystallization is less pronounced.

The volcanism in the region generated and evolved under the influence of the roll-back / rotation of the Hellenic slab and the pathways generated by the subsequent tectonic structures (İBTZ, core complex formation of Menderes Massif).

Supplementary Materials: The following are available online at www.mdpi.com/xxx/s1, Supplementary Table 1: Results of LA-ICP-MS U–Pb zircon ages of samples, Supplementary Table 2: Whole-rock major (wt.%), trace (ppm) and rare earth elements (REE) (ppm) results of the studied volcanic rocks.

Author Contributions: For research articles with several authors, a short paragraph specifying their individual contributions must be provided. The following statements should be used “Conceptualization, A.İ.. and N.A.; methodology, A.İ., N.A.; validation, A.İ..; formal analysis, A.İ..; investigation, A.İ., N.A.; resources, A.İ., N.A.; data curation, A.İ.,; writing—original draft preparation, A.İ., N.A..; writing—review and editing, A.İ., N.A.; visualization, A.İ.; supervision, N.A.; project administration, A.İ.; funding acquisition, A.İ. All authors have read and agreed to the published version of the manuscript.”, please turn to the CRediT taxonomy for the term explanation. Authorship must be limited to those who have contributed substantially to the work reported.

Acknowledgments: We thank reviewers and the Editor for their constructive comments.

Conflicts of Interest: The authors declare no conflict of interest. The funders had no role in the design of the study; in the collection, analyses, or interpretation of data; in the writing of the manuscript, or in the decision to publish the results.

References

1. Jolivet, L., Faccenna, C., Huet, B., Labrousse, L., Le Pourhiet, L., Lacombe, O., Philippon, M. *Aegean tectonics: Strain localisation, slab tearing and trench retreat.* Tectonophysics 2013, 597, 1-33.
2. Delaloye, M.; Bingöl, E. *Granitoids from western and northwestern Anatolia: geochemistry and modeling of geodynamic evolution.* International Geology Review 2000, *42*, 241-268.
3. Köprübaşı, N.; Aldanmaz, E. *Geochemical constraints on the petrogenesis of Cenozoic I-type granitoids in Northwest Anatolia, Turkey: evidence for magma generation by lithospheric delamination in a post-collisional setting.* International Geology Review 2004, *46*, 705-729.
4. Ustaömer, P. A., Ustaömer, T., Collins, A.S., *Reischpeitsch, J. Lutetian arc-type magmatism along the southern Eurasian margin: new U-Pb LA-ICPMS and whole-rock geochemical data from Marmara Island, NW Turkey.* Mineralogy and Petrology 2009, *96*, 177-196.
5. Altunkaynak, Ş., Sunal, G., Aldanmaz, E., Genç, C.Ş., Dilek, Y., Furnes, H., Yıldız, M. *Eocene granitic magmatism in NW Anatolia (Turkey) revisited: new implications from comparative zircon SHRIMP U–Pb and 40Ar–39Ar geochronology and isotope geochemistry on magma genesis and emplacement.* Lithos 2012, *155*, 289-309.
6. Ersoy, E.Y., Palmer, M.R. *Eocene-Quaternary magmatic activity in the Aegean: Implications for mantle metasomatism and magma genesis in an evolving orogeny.* Lithos 2013, *180*, 5-24.
7. Aldanmaz, E., Pearce, J.A., Thirlwall, M. F., Mitchell, J.G. *Petrogenetic evolution of late Cenozoic, post-collision volcanism in western Anatolia, Turkey.* Journal of volcanology and geothermal research 2000, *102*, 67-95.
8. Ersoy, E.Y., Helvacı, C., Palmer, M.R. *Mantle source characteristics and melting models for the early-middle Miocene mafic volcanism in Western Anatolia: implications for enrichment processes of mantle lithosphere and origin of K-rich volcanism in postcollisional settings*. J. Volcanol. Geotherm. Res. 2010, *198*, 112–128.
9. Altunkaynak, Ş., Dilek, Y., Genç, C.Ş., Sunal, G. Gertisser, R. Furnes, H. Yang, J. *Spatial, temporal and geochemical evolution of Oligo–Miocene granitoid magmatism in western Anatolia, Turkey*. Gondwana Research 2012, *21*, 961-986.
10. Aysal, N. *Mineral chemistry, crystallization conditions and geodynamic implications of the Oligo–Miocene granitoids in the Biga Peninsula, Northwest Turkey.* Journal of Asian Earth Sciences 2015, *105*, 68-84.
11. Ercan, T., Satır, M., Sevin, D., Türkecan, A. *Batı Anadolu'daki Tersiyer ve Kuvaterner yaşlı volkanik kayaçlarda yeni yapılan radyometrik yaş ölçümlerinin yorumu (Some new radiometric ages from Tertiary and Quaternary volcanic rocks fromWest Anatolia).* Bull. Miner. Res. Explor. Inst. Turk. 1996, *119*, 103–112.
12. Ersoy, E.Y., Helvacı, C., Uysal, İ., Karaoğlu, Ö., Palmer, M.R., Dindi, F. *Petrogenesis of the Miocene volcanism along the İzmir–Balıkesir Transfer Zone in western Anatolia, Turkey: implications for origin and evolution of potassic volcanism in postcollisional areas.* J. Volcanol. Geotherm. Res. 2012, *241–242*, 21–38.
13. Uzel, B., Sözbilir, H., Özkaymak, Ç., Kaymakcı, N., Langereis, C.G. *Structural evidence for strike-slip deformation in the İzmir–Balıkesir transfer zone and consequences for late Cenozoic evolution of western Anatolia (Turkey).* Journal of Geodynamics 2013, *65*, 94-116.
14. Karaoğlu, Ö. *Tectonic controls on the Yamanlar volcano and Yuntdağı volcanic region, western Turkey: Implications for an incremental deformation.* Journal of Volcanology and Geothermal Research 2014, *274*, 16–33.
15. Üşümezsoy, Ş. *Evolution of the NW Anatolian Pb-Zn deposits: litospheric detachment in compressional and extensional regime in NW Anatolian accretionary belt magmatism and metallogenesis.* Geosound 1988, *177*, 1–34.
16. Emre, T., and Sözbilir, H. *Field evidence for metamorphic core complex, detachment faulting and accommodation faults in the Gediz and Büyük Menderes grabens, western Anatolia*. IESCA-1995 Proceedings 1, 73–93.
17. Gessner, K., Ring, U., Johnson, C., Hetzel, R., Passchier, C. W., Güngör, T. *An active bivergent rolling-hinge detachment system: Central Menderes metamorphic core complex in western Turkey*. Geology 2001, *29 (7)*, 611-614.

18. Erkül, F., Helvaci, C., Sözbilir, H. *Stratigraphy and Geochronology of the Early Miocene Volcanic Units in the Bigadiç Borate Basin, Western Turkey.* Turkish Journal of Earth Sciences 2005, *14 (3)*, 227-253.
19. Van Hinsbergen, D. J., Dekkers, M. J., Bozkurt, E., Koopman, M. *Exhumation with a twist: Paleomagnetic constraints on the evolution of the Menderes metamorphic core complex, western Turkey.* Tectonics 2010, *29*, 1-33.
20. Ring, U., Glodny, J., Will, T., Thomson, S. *The Hellenic subduction system: high-pressure metamorphism, exhumation, normal faulting, and large-scale extension.* Annual Review of Earth and Planetary Sciences 2010, *38*, 45-76.
21. Tokçaer, M., Agostini, S., Savaşçin, M.Y. *Geotectonic setting and origin of the youngest Kula volcanics (western Anatolia), with a new emplacement model.* Turkish Journal of Earth Sciences 2005, *14 (2)*, 143-166.
22. Grützner, T., Prelević, D., Akal, C. *Geochemistry and origin of ultramafic enclaves and their basanitic host rock from Kula Volcano, Turkey.* Lithos 2013, *180*, 58-73.
23. Uzel, B., Kuiper, K., Sözbilir, H., Kaymakci, N., Langereis, C.G., Boehm, K. *Miocene geochronology and stratigraphy of western Anatolia: Insights from new Ar/Ar dataset.* Lithos 2020, *352*, 105305.
24. Uzel, B.; Sözbilir, H. *A First record of strike-slip basin in western Anatolia and its tectonic implication: The Cumaovası basin as an example.* Turk. J. Earth Sci. 2008, *17*, 559-591.
25. Liu Y, Hu Z, Zong K, Gao C, Gao S., Xu, J., Chen, H. *Reappraisement and refinement of zircon U-Pb isotope and trace element analyses by LA-ICP-MS*. Chinese Science Bulletin 2010, *55 (15)*, 1535-1546.
26. Okay, A.I.; Altıner, D. *A condensed Mesozoic section in the Bornova Flysch Zone: A fragment of the Anatolide-Tauride carbonate platform.* Turkish Journal of Earth Sciences 2007, *16*, 257-279.
27. Okay, A. I.; İşintek, İ.; Altıner, D.; Özkan-Altıner, S.; Okay, N. *An olistostrome–mélange belt formed along a suture: Bornova Flysch zone, western Turkey*. Tectonophysics 2012, *568*, 282-295.
28. Brinkmann, R. *Geotektonische gliederung von VVestanatolien (Stuttgart)*. N.Jb. Geol. Palaont Mh 1966, *10*, 603-618.
29. Erdoğan, B. *İzmir-Ankara Zonu'nun İzmir-Seferihisar arasındaki bölgede stratigrafik özellikleri ve tektonik evrimi.* TP Jeologları Derneği Bülteni 1990, *2/1*, 1-20.
30. Akay, E.; Erdoğan, B. *Evolution of Neogene calc-alkaline to alkaline volcanism in the Aliağa-Foça region (Western Anatolia, Turkey).* Journal of Asian Earth Sciences 2004, *24*, 367-387.
31. Altunkaynak, Ş.; Rogers, N. W.; Kelley, S. P. *Causes and effects of geochemical variations in late Cenozoic volcanism of the Foça volcanic centre, NW Anatolia, Turkey.* International Geology Review 2010, *52*, 579-607.
32. Kaya, O. *Ege kıyı kuşağı (Dikili-Zeytindağı-Menemen-Yenifoça) Neojen stratigrafisi.* EÜ Fen Fakültesi 1978, pn. 17.
33. Hasözbek, A. *Dursunbey (Balıkesir)-Foça (İzmir) Erken-Orta Miyosen Volkaniklerinin İzotop Jeokimyası.* D.Ü. Mühendislik Fakültesi Fen ve Mühendislik Dergisi 2017, *19*, 950-967.
34. Dönmez, M., Akçay, A.E., Türkecan, A. *Batı Anadolu'da yeni bir kaldera: Foça kalderası.* Doğal Kaynaklar ve Ekonomi Bülteni 2017, *24*, 13-20.
35. Akçay, A. E., Dönmez, M., Türkecan, A. *Türkiye jeoloji haritaları, URLA-K17 paftası.* MTA Genel Müdürlüğü Yayını 2014, n.212.
36. Akyürek, B., Soysal, Y. *Kırkağaç-Soma (Manisa)-Savaştepe, Korucu, Ayvalık (Balıkesir)-Bergama (İzmir) civarının jeolojisi.* MTA Enstitüsü (unpublished) 1978, rn. 6432.
37. Dönmez, M., Türkecan, A., Akçay, A.E., Hakyemez, Y., Sevin, D. *İzmir ve kuzeyinin jeolojisi Tersiyer volkanizmasının petrografik ve kimyasal özellikleri.* MTA Genel Müdürlüğü (yayımlanmamış) 1998, pn. 10181.
38. Dönmez, M., Akçay, A.E., Türkecan, A. *1/100 000 ölçekli Türkiye Jeoloji Haritaları, İzmir K18 Paftası*, MTA Genel Müdürlüğü 2014, n. 23.
39. Türkecan, A. *Türkiye'nin Senozoyik Volkanitleri*. MTA Genel Müdürlüğü Özel Yayın Serisi 2015, n. 33.
40. Eşder, T., Yakabağ, A., Sarıkaya, H., Çiçekli, K. *Aliağa (İzmir) yöresinin jeolojisi ve jeotermal enerji olanakları*. MTA Genel Müdürlüğü (yayımlanmamış) 1991, n. 9467.
41. Ercan, T., Satır, M., Kreuzer, H., Türkecan, A., Günay, E., Çevikbaş, A., Ateş, M., Can, B. *Batı Anadolu Senozoyik volkanitlerine ait yeni kimyasal, izotopik ve radyometrik verilerin yorumu (The interpretation of new chemical, isotopic and geochronologic data from the Cenozoic volcanics of western Turkey).* Bull. Geol. Soc. of Turk. 1985, *28*, 121–136.

42. Winchester, J.A., and Floyd, P.A. *Geochemical discrimination of different magma series and their differentiation products using immobile elements.* Chemical geology, 1977, *20*, 325-343.
43. Peccerillo, A., and Taylor, S.R. *Geochemistry of Eocene calc-alkaline volcanic rocks from the Kastamonu area, northern Turkey*. Contributions to mineralogy and petrology, 1976, *58*, 63-81.
44. Seghedi, I., Helvacı, C. *Early Miocene Kırka-Phrigian Caldera, western Turkey (Eskişehir province), preliminary volcanology, age and geochemistry data*. Journal of Volcanology and Geothermal Research 2016, *327*, 503-519.
45. Keskin, M., FC-modeler: *A Microsoft® Excel© spreadsheet program for modeling Rayleigh fractionation vectors in closed magmatic systems*. Computers and Geosciences 2002, *28*, 919–928.
46. DePaolo, D.J. *Trace element and isotopic effects of combined wallrock assimilation and fractional crystallization.* Earth and planetary science letters 1981, *53*, 189-202.
47. Keskin, M., AFC-Modeler: *A Microsoft® Excel© Workbook Program for Modelling Assimilation combined with Fractional Crystallization (AFC) Process in Magmatic Systems by Using Equations of DePaolo (1981).* Turkish Journal of Earth Sciences, 2013, *22*, 304-319.
48. Taylor, S.R., and McLennan, S.M. *The continental crust: its composition and evolution* United States: N. p., 1985.
49. Sun, S.S., MacDonough, W.F. *Chemical and isotopic systematics of oceanic basalts: Implications for mantle composition and processes.* Geological Society of London Special Publication 1989, *42*, 313–345.
50. Pearce, J.A., Harris, N.B., Tindle, A.G. *Trace element discrimination diagrams for the tectonic interpretation of granitic rocks.* Journal of petrology 1984, *25*, 956-983.
51. Harris, M., Mackender, R.O., Smith, D.L. *Photosynthesis of cotyledons of soybean seedlings*. New Phytologist 1986, *104*, 319-329.
52. Schandl, E.S.; Gorton, M.P. *Application of high field strength elements to discriminate tectonic settings in VMS environments.* Economic geology 2002, *97*, 629-642.
53. Pearce, J.A. *Geochemical fingerprinting of oceanic basalts with applications to ophiolite classification and the search for Archean oceanic crust*. Lithos 2008, *100*, 14-48.
54. Borsi, S., Ferrara, G., Innocenti, F., Mazzuoli, R. *Geochronology and petrology of recent volcanics in the Eastern Aegean Sea (West Anatolia and Lesvos Island).* Bulletin Volcanologique 1972, *36*, 473-496.
55. Fytikas, M., Giuliani, O., Innocenti, F., Marinelli, G., Mazzuoli, R. *Geochronological data on Recent magmatism of the Aegean Sea.* Tectonophysics 1976, *31*, 29-34.
56. Akal, C. *Mechanism of emplacement and origin of the Ildır lava dome in the Karaburun Peninsula, western Anatolia (Turkey)*. Journal of Asian Earth Sciences 2019, *179*, 80-98.
57. Ersoy, E.Y., Palmer, M.R., Genç, Ş.C., Prelević, D., Akal, C., Uysal, İ. *Chemo-probe into the mantle origin of the NW Anatolia Eocene to Miocene volcanic rocks: implications for the role of subduction, slab roll-back and slab break-off processes in genesis of post-collisional magmatism*. Lithos 2017, *288–289*, 55–71.
58. Fytikas, M., Innocenti, F., Manetti, P., Peccerillo, A., Mazzuoli, R., Villari, L. *Tertiary to Quaternary evolution of volcanism in the Aegean region.* Geological Society, London, Special Publications 1984, *17*, 687-699.
59. Pe-Piper, G., Piper, D.J. *Spatial and temporal variation in Late Cenozoic back-arc volcanic rocks, Aegean Sea region.* Tectonophysics 1989, *169*, 113-134.
60. Innocenti, F., Agostini, S., Di Vincenzo, G., Doglioni, C., Manetti, P., Savaşçın, M.Y., Tonarini, S. *Neogene and Ouaternary volcanism in VVestern Anatolia: Magma sources and geodynamic evolution*. Marine Geology 2005, *221*,397-421.